Inorg. Chem. **2008**, *47*, 10446−10454

Synthesis and Characterization of Dicyclopalladated Complexes of Azobenzene Derivatives by Experimental and Computational Methods

Darko Babić,*,† Manda Ćurić,† Krešimir Molčanov,† Gregor Ilc,‡ and Janez Plavec‡

Institute "Ruđer Bošković", Bijenička 54, HR-10002 Zagreb, Croatia, and Slovenian NMR Center, National Institute of Chemistry, Hajdrihova 19, SI-1000 Ljubljana, Slovenia

Received June 3, 2008

A series of doubly cyclopalladated complexes of azobenzene and its unsymmetrical substituted derivatives, namely, {LPdCl(μ-AZB)LPdCl}, where AZB is azobenzene, 4-methylazobenzene, 4-aminoazobenzene, or 4-(dimethylamino)-4′-nitroazobenzene, while L is N,N-dimethylformamide, dimethylsulfoxide, or pyridine, have been prepared. Their structural and spectroscopic properties were determined by X-ray diffraction analysis as well as by ^{1}H NMR, IR, UV−vis, and fluorimetric studies. Experimental results were rationalized by quantum chemical calculations. Crystal structures of several complexes have been resolved, and for the first time, it was demonstrated that the cyclopalladation may take place at the azobenzene aromatic ring having the strong electron-withdrawing substituent at the para position. In all cases, the metalated carbon and N,N-dimethylformamide or dimethylsulfoxide ligands are mutually trans, whereas the pyridine ligands are in the cis arrangement. cis/trans isomerism in the isolated compounds is explained by comparing the calculated energies of isomeric structures. All of the complexes absorb strongly in the visible region, and according to time-dependent density functional theory calculations, most of the absorptions can be attributed to intraligand $\pi \rightarrow \pi^*$ or metal-to-ligand charge-transfer transitions. The fluorescence emission was observed for the complexes with 4-aminoazobenzene or 4-(dimethylamino)-4′-nitroazobenzene. The aromaticity of palladacycles is evaluated by several aromaticity indices and related to relevant experimental findings.

Introduction

In contrast to a number of monocyclopalladated azobenzene complexes,[1] a convenient preparation of doubly cyclopalladated species has been reported only recently.[2] Since these azobenzene complexes have two metalated phenyl rings, they are promising candidates for much wider application in the organic synthesis and catalysis than their singly cyclopalladated analogues. Some monocyclopalladated complexes of azobenzenes were found to display mesogenic, photoconducting, photorefractive, and luminescence properties.[3] Those properties were attributed to the 4,4′-substituents and to the aromaticity of the fused phenyl ring and the five-membered palladacycle.[3] In doubly cyclopalladated azobenzenes, the size of the aromatic system should be increased in comparison with the monocyclopalladated ones. Furthermore, doubly cyclopalladated complexes may form bridged associates on both sides and thus serve as basic units for designing a wide variety of organometallic polymers and more elaborate supramolecular systems.[4]

* Author to whom correspondence should be addressed. E-mail: dbabic@irb.hr.
† Institute "Ruđer Bošković".
‡ National Institute of Chemistry.

(1) (a) Cope, A. C.; Siekman, R. W. *J. Am. Chem. Soc.* **1965**, *87*, 3272. (b) Takahashi, H.; Tsuji, J. *J. Organomet. Chem.* **1967**, *10*, 511. (c) Parshall, G. W. *Acc. Chem. Res.* **1970**, *3*, 139. (d) Dehand, J; Pfeffer, M. *Coord. Chem. Rev.* **1976**, *18*, 327. (e) Bruce, M. I. *Angew. Chem., Int. Ed.* **1977**, *16*, 73. (f) Bruce, M. I.; Goodall, B.; Stone, G. A. *J. Chem. Soc., Dalton Trans.* **1978**, 687. (g) Omae, I. *Chem. Rev.* **1979**, *79*, 267; *Coord. Chem. Rev.* **2004**, *248*, 995. (h) Wakatsuki, Y.; Yamazaki, H.; Grutsch, P. A.; Santhanam, M.; Kutal, C. *J. Am. Chem. Soc.* **1985**, *107*, 8153. (i) Ryabov, A. D. *Synthesis* **1985**, 233. (j) Mahapatra, A. K.; Bandyopadhyay, D.; Bandyopadhyay, P.; Chakravorty, A. *Inorg. Chem.* **1986**, *25*, 2215. (k) Sinha, C.; Bandyopadhyay, D.; Chakravorty, A. *Inorg. Chem.* **1988**, *27*, 1173. (l) Ghedini, M.; Pucci, D.; Crispini, A.; Barberio, G.; Aiello, I.; Barigelletti, F.; Gessi, A.; Francescangeli, O. *Appl. Organomet. Chem.* **1999**, *13*, 565. (m) Ćurić, M.; Babić, D.; Marinić, Ž.; Paša-Tolić, Lj.; Butković, V.; Plavec, J.; Tušek-Božić, Lj. *J. Organomet. Chem.* **2003**, *687*, 85. (n) Dupont, J.; Consorti, C. S.; Spencer, J. *Chem. Rev.* **2005**, *105*, 2527.

(2) Ćurić, M.; Babić, D.; Višnjevac, A.; Molčanov, K. *Inorg. Chem.* **2005**, *44*, 5975.

(3) Ghedini, M.; Aiello, I.; Crispini, A.; Golemme, A.; La Deda, M.; Pucci, D. *Coord. Chem. Rev.* **2006**, 1373.

10.1021/ic8010234 CCC: $40.75
Published on Web 10/23/2008

This paper presents the synthesis and characterization of a new set of doubly cyclopalladated complexes with azobenzenes, as well as the discussion and rationalization of their structural and spectroscopic properties. The experimental results were complemented by theoretical calculations in order to explain cis/trans isomerism in isolated complexes, their aromaticity, and the nature of the electronic transitions.

Experimental Section

All chemicals and solvents used for the syntheses were commercially available. Complexes **1a**,**b** and **3a**,**b** have been prepared following the reported procedures.[2] UV−vis absorption bands in dimethylsulfoxide (DMSO), λ_{max}/nm ($\varepsilon/10^4$ M^{-1} cm^{-1}), of **1b** are as follows: 318 (0.76), 404 (1.5), 445 sh (0.75), 553 (0.43), 586 (0.46). Those of **3b** are as follows: 307 (1.6), 381 (1.3), 432 sh (0.92), 466 sh (0.77), 530 sh (1.0), 615 sh (2.6), 639 (2.7).

{PdCl(DMF)(μ-$C_6H_4N{=}NC_6H_3CH_3$)PdCl(DMF)}(2a) and {PdCl(DMF)(μ-$O_2NC_6H_3N{=}NC_6H_3N(CH_3)_2$)-PdCl(DMF)} (4a). Complexes **2a** and **4a** were prepared following a similar procedure as described for **1a** (or **3a**)[2] starting with 50 mg (0.26 mmol) of 4-methylazobenzene (**mab**) and 330 mg (1.27 mmol) of $PdCl_2(CH_3CN)_2$ for **2a** and 50 mg (0.19 mmol) of 4-(dimethylamino)-4′-nitroazobenzene (**dmanab**) and 240 mg (0.93 mmol) of $PdCl_2(CH_3CN)_2$ for **4a** dissolved in 7 mL of dimethylformamide (DMF). **2a**. Yield 75%. Anal. calcd (found) for $C_{19}H_{24}N_4O_2Pd_2Cl_2$: C, 36.56 (36.95); H, 3.85 (4.40); N, 9.00 (8.65). **4a**. Yield 60%. Anal. calcd (found) for $C_{20}H_{26}N_6O_4Pd_2Cl_2$: C, 34.40 (34.90); H, 3.73 (3.25); N, 12.04 (11.55).

{PdCl(DMSO)(μ-$C_6H_4N{=}NC_6H_3CH_3$)PdCl(DMSO)} (2b) and {PdCl(DMSO)(μ-$O_2NC_6H_3N{=}NC_6H_3N(CH_3)_2$)PdCl(DMSO)} (4b). Complexes **2b** and **4b** were prepared by similar procedures. A total of 100 mL of a solution of complex **2a** (50 mg, 0.08 mmol) and 40 mL of a solution of complex **4a** (50 mg, 0.07 mmol), respectively, in DMSO were filtered off and concentrated to 20 mL (**2a**) and to 5 mL (**4a**). The red and brown-red crystals of **2b** and **4b**, respectively, were obtained. **2b**. Yield 65%. Anal. calcd (found) for $C_{17}H_{22}N_2S_2O_2Pd_2Cl_2$: C, 32.19 (31.72); H, 3.47 (3.70); N, 4.42 (4.00). ^{1}H NMR (DMSO-d_6): δ 7.68 s (H-3), 7.06 d (H-5, ^3J(HH) = 7.7 Hz), 8.64 d (H-6, ^3J(HH) = 7.8 Hz), 7.84 d (H-9, ^3J(HH) = 7.6 Hz), 7.16 t (H-10, ^3J(HH) = 7.6 Hz), 7.22 t (H-11, ^3J(HH) = 7.6 Hz), 8.69 d (H-12, ^3J(HH) = 7.5 Hz), 3.11 s (−C**H**$_3$). UV−vis (DMSO) λ_{max}/nm ($\varepsilon/10^4$ M^{-1} cm^{-1}): 314 (0.63), 406 (1.5), 447 sh (0.77), 555 (0.51), 589 (0.55). **4b**. Yield 43%. Anal. calcd (found) for $C_{18}H_{24}N_4S_2O_4Pd_2Cl_2$: C, 30.51 (29.98); H, 3.40 (3.48); N, 7.91 (8.38). ^{1}H NMR (DMSO-d_6): δ 7.30 s (H-3), 6.81 d (H-5, ^3J(HH) = 9.4 Hz), 8.35 d (H-6, ^3J(HH) = 9.3 Hz), 8.43 s (H-9), 7.94 d (H-11, ^3J(HH) = 9.2 Hz), 8.59 d (H-12, ^3J(HH) = 9.2 Hz), 3.33 s (−C**H**$_3$)$_2$. UV−vis (DMSO) λ_{max}/nm ($\varepsilon/10^4$ M^{-1} cm^{-1}): 308 (1.1), 386 (1.0), 456 (0.62), 495 sh (0.46), 641 sh (2.6), 671 sh (3.0), 695 (3.3).

{PdCl(py)(μ-$C_6H_4N{=}NC_6H_4$)PdCl(py)} (1c) and {PdCl(py)-(μ-$C_6H_4N{=}NC_6H_3CH_3$)PdCl(py)} (2c). Complexes **1c** and **2c** were prepared by dissolving complex **1a** (50 mg, 0.08 mmol) and **2a** (50 mg, 0.08 mmol), respectively, in pyridine (py; 20 mL for **1a** and 15 mL for **2a**), and these were allowed to stand at room temperature for a day. The red and brown-red crystals of **1c** and **2c**, respectively, were obtained. **1c**. Yield 68%. Anal. calcd (found) for $C_{22}H_{18}N_4Pd_2Cl_2$: C, 42.46 (42.18); H, 2.90 (3.25); N, 9.01 (8.98). **2c**. Yield 62%. Anal. calcd (found) for $C_{23}H_{20}N_4Pd_2Cl_2$: C, 43.42 (43.03); H, 3.15 (2.71); N, 8.81 (8.38).

{PdCl(py)(μ-$C_6H_4N{=}NC_6H_3NH_2$)PdCl(py)} (3c). Complex **3a** (50 mg, 0.08 mmol) was suspended in diethyl ether (15 mL), and py (0.1 mL) was added. The resulting mixture was stirred at 25 °C for 3 h. The brown-red precipitate was filtered off and dried under a vacuum. Yield 71%. Anal. calcd (found) for $C_{22}H_{19}N_5Pd_2Cl_2$: C, 41.46 (41.13); H, 3.00 (2.94); N 11.00 (10.58).

{PdCl(py)(μ-$O_2NC_6H_3N{=}NC_6H_3N(CH_3)_2$)PdCl(py)} (4c). Complex **4a** (50 mg, 0.07 mmol) was dissolved in py (60 mL). The solution was filtered off, and hexane was added to precipitate **4c** as brown-red crystals. Yield 74%. Anal. calcd (found) for $C_{24}H_{22}N_6O_2Pd_2Cl_2$: C, 40.58 (41.07); H, 3.10 (3.13); N, 11.84 (11.61).

General Methods. NMR spectra were acquired on Bruker AV-600 and Varian VNMRS 600 MHz spectrometers using a 5 mm high-resolution triple-resonance probe with gradients (^{1}H at 599.81 MHz). All spectra were acquired in DMSO-d_6 or in DMF-d_7 at room temperature. Individual resonances were assigned on the basis of their chemical shifts, signal intensities, and a multiplicity of resonances as well as on the ^{1}H−^{1}H correlation spectroscopy experiments. IR spectra were recorded on an AAB Bomem MB 102 spectrophotometer using KBr and CsI pellets (4000−200 cm^{-1}). Electronic absorption spectra were recorded on a Hewlett-Packard 8452A spectrophotometer with a thermostatted cell compartment at 25 °C. Luminescence spectra where taken on a Varian Eclipse spectrophotometer at 25 °C. X-ray powder diffraction data were obtained using Cu Kα radiation (λ = 1.5406 Å) on a Philips PW 1710 diffractometer.

X-Ray Structure Analysis. All crystallographic measurements were done at room temperature. Data for compounds **1c**, **2a**, **2b**, and **4b** were collected on an Enraf-Nonius CAD4 diffractometer, using a graphite monochromated Cu Kα (1.54179 Å) radiation. The WinGX standard procedure was applied for data reduction.[5] Three standard reflections were measured every 120 min as an intensity control. Absorption correction based on eight ψ-scan reflections[6] was applied. Structure **4a** was measured in an Oxford Diffraction Xcalibur Nova diffractometer with a microfocusing tube (Cu Kα radiation). The CrysAlis PRO program package[7] was used for data reduction and multiscan absorption correction. The structures were solved with SHELXS97[8] and refined with SHELXL97.[9] The models were refined using full matrix least-squares refinement. Hydrogen atoms were treated as riding entities. The atomic scattering factors were those included in SHELXL97. Molecular geometry calculations were performed with PLATON,[10] and molecular graphics were prepared using ORTEP-3[11] and CCDC-Mercury.[12] Crystallographic and refinement data for the reported structures are shown in Table 1.

Supplementary crystallographic data for this paper can be obtained free of charge via http://www.ccdc.cam.ac.uk/conts/

(4) (a) Loeb, S. J.; Shimizu, G. K. H. *J. Chem. Soc., Chem. Commun* **1993**, 1395. (b) Ye, B. H.; Tong, M. L.; Chen, X. M. *Coord. Chem. Rev.* **2005**, *249*, 545. (c) Janiak, C. *J. Chem. Soc., Dalton Trans.* **2000**, 3885.

(5) Harms, K.; Wocadlo, S. *XCAD-4*; University of Marburg: Marburg, Germany, 1995.

(6) North, A. C. T.; Philips, D. C.; Mathews, F. S. *Acta Crystallogr., Sect. A* **1968**, *24*, 351.

(7) *CrysAlis PRO*; Oxford Diffraction Ltd.: Oxford, U. K.

(8) Sheldrick, G. M. *SHELX97*, release 97-2; University of Göttingen: Göttingen, Germany, 1997.

(9) Sheldrick, G. M. *SHELXL97*; Universität Göttingen: Göttingen, Germany, 1997.

(10) Spek, A. L. *PLATON98: A Multipurpose Crystallographic Tool*,, 120398 Version; University of Utrecht: Utrecht, The Netherlands, 1998.

(11) Farrugia, L. J. *J. Appl. Crystallogr.* **1997**, *30*, 565.

(12) McCabe, P.; Pidcock, E.; Shields, G. P.; Taylor, R; Towler, M.; Macrae, C. F.; Edgington, P. R.; Van de Streek, J. *J. Appl. Crystallogr.* **2006**, *39*, 453.

Table 1. Crystallographic Data and Structure Refinement Data for Compounds **1c**, **2a**,**b**, and **4a**,**b**

compound	**1c**	**2a**	**2b**	**4a**	**4b**
empirical formula	$C_{22}H_{18}Cl_2N_4Pd_2$	$C_{19}H_{24}N_4Cl_2O_2Pd_2$	$C_{18}H_{24}Cl_2N_2O_2Pd_2S_2$	$C_{20}H_{26}Cl_2N_6O_4Pd_2$	$C_{18}H_{24}Cl_2N_4O_4Pd_2S_2$
fw/g mol^{-1}	622.16	624.12	648.21	698.21	708.29
cryst dimensions/mm	0.20 × 0.05 × 0.05	0.10 × 0.01 × 0.01	0.10 × 0.03 × 0.03	0.23 × 0.08 × 0.03	0.18 × 0.07 × 0.03
space group	$P2_1/n$	$P2_1/c$	$P\bar{1}$	$P2_1/c$	$P2_1/n$
a/Å	5.2111(11)	12.689(5)	6.5629(4)	14.1137(8)	12.8502(6)
b/Å	17.221(3)	5.5253(7)	7.2720(3)	14.1118(6)	7.3983(9)
c/Å	12.1709(12)	31.142(6)	12.5433(6)	13.8309(7)	26.052(2)
α/deg	90	90	87.916(4)	90	90
β/deg	102.032(14)	92.75(3)	81.087(4)	114.600(6)	103.010(5)
γ/deg	90	90	67.428(4)	90	90
Z	2	4	1	4	4
V/Å^3	1068.2(3)	2180.9(10)	545.93(5)	2504.7(2)	2413.2(4)
D_{calcd}/g cm^{-3}	1.934	1.901	1.972	1.852	1.950
μ/mm^{-1}	16.019	15.756	17.476	13.886	15.973
Θ range/deg	4.52−76.15	2.84−75.69	3.57−76.37	3.12−75.94	53.48−78.2
range of h, k, l	$-6 > h > 0$; $0 > k > 21$; $-14 > l > 15$	$-15 > h > 15$; $-6 > k > 0$; $-39 > l > 0$	$-8 > h > 7$; $-9 > k > 0$; $-15 > l > 15$	$-16 > h > 17$; $-15 > k > 17$; $-17 > l > 17$	$0 > h > 16$; $0 > k > 9$; $-32 > l > 32$
reflns collected	2470	4599	2486	14813	5330
ind reflns	2227	4510	2298	5078	5098
obsd reflns ($I \geq 2\sigma$)	1132	1930	1913	3700	2042
R_{int}	0.0844	0.0714	0.0155	0.0433	0.1238
R (F)	0.0703	0.078	0.0409	0.0604	0.0842
R_w (F^2)	0.1756	0.1544	0.1133	0.173	0.2024
goodness of fit	0.980	1.022	1.106	1.082	0.976
no. of params	136	243	130	307	289
$\Delta\rho_{max}$; $\Delta\rho_{min}$ (e Å^{-3})	0.852; −0.939	1.097; −1.383	0.102; −1.03	1.418; −0.549	1.093; −1.575

retrieving.html (or from the Cambridge Crystallographic Data Centre, 12, Union Road, Cambridge CB2 1EZ, U. K.; fax, +44 1223 336033; e-mail, deposit@ccdc.cam.ac.uk). CCDC 684829−684833 contain the supplementary crystallographic data for this paper.

Computational Methods. Calculations were performed with Gaussian 03;[13] only geometry optimization in a solvent was done with Jaguar.[14] Geometries were tightly optimized by the DFT method with the B3LYP[15] functional and 6-31G(d,p) basis set on all nonmetal atoms plus the Stuttgart−Dresden effective core potential and basis set[16] (SDD) on Pd atoms. Stationary points were confirmed as minima by Hessian eigenvalues. Solvation effects were estimated by the Poisson−Boltzmann model[17] implemented in Jaguar, with dielectric constants and solvent radii for DMF: ε = 36.7, r = 2.481 Å; for DMSO: ε = 46.7, r = 2.455 Å; and for py: ε = 12.4, r = 2.518 Å. The calculated IR spectrum of **1a** was linearly scaled and shifted so as to produce the best agreement with the experimental spectrum. The same scaling/shifting was applied to the calculated spectrum of the T-shaped complex.

Vertical excitation energies and oscillatory strengths were calculated by time-dependent DFT (TD-DFT) with the B3LYP functional and 6-311+G(d,p) basis on all atoms except on Pd, for which the SDD pseudopotential was used and the SDD basis set was augmented by additional s, p, d, and f basis functions with exponents α(s) = 0.008, α(p) = 0.012, α(d) = 0.03, and α(f) = 1.47, as reccommended in the literature.[18] The solvation effect on electronic wave function was accounted for by the PCM model with parameters for DMSO and UA0 atomic radii.[13]

Results and Discussion

Synthesis of Complexes. We have previously reported the synthesis of complexes **1a**,**b** and **3a**,**b** (Scheme 1).[2] The new complexes (**2a**,**b** and **4a**,**b** and **1c**−**4c**) were obtained by similar procedures, presented in Scheme 1. All compounds were isolated as crystalline solids, soluble in DMF, DMSO and py, while complexes **1c**−**4c** are also slightly soluble in polar solvents with poor coordinating ability (CH_2Cl_2, $CHCl_3$, EtOH, and MeOH). Complex **3c** is sparingly soluble in H_2O too. All complexes contain two solvent ligands (DMF, DMSO, or py) which are interchangeable (Scheme 1).

In contrast to the coordinated py molecules, coordinated molecules DMF or DMSO can be removed by washing complexes with H_2O, EtOH, and CH_2Cl_2, resulting in dark, noncrystalline species, as detected by X-ray powder diffraction. The initial complexes were restored by dissolving these species in DMF or DMSO. Their IR (Supporting Information

(13) Frisch, M. J.; Trucks, G. W.; Schlegel, H. B.; Scuseria, G. E.; Robb, M. A.; Cheeseman, J. R.; Montgomery, J. A., Jr.; Vreven, T.; Kudin, K. N.; Burant, J. C.; Millam, J. M.; Iyengar, S. S.; Tomasi, J.; Barone, V.; Mennucci, B.; Cossi, M.; Scalmani, G.; Rega, N.; Petersson, G. A.; Nakatsuji, H.; Hada, M.; Ehara, M.; Toyota, K.; Fukuda, R.; Hasegawa, J.; Ishida, M.; Nakajima, T.; Honda, Y.; Kitao, O.; Nakai, H.; Klene, M.; Li, X.; Knox, J. E.; Hratchian, H. P.; Cross, J. B.; Bakken, V.; Adamo, C.; Jaramillo, J.; Gomperts, R.; Stratmann, R. E.; Yazyev, O.; Austin, A. J.; Cammi, R.; Pomelli, C.; Ochterski, J. W.; Ayala, P. Y.; Morokuma, K.; Voth, G. A.; Salvador, P.; Dannenberg, J. J.; Zakrzewski, V. G.; Dapprich, S.; Daniels, A. D.; Strain, M. C.; Farkas, O.; Malick, D. K.; Rabuck, A. D.; Raghavachari, K.; Foresman, J. B.; Ortiz, J. V.; Cui, Q.; Baboul, A. G.; Clifford, S.; Cioslowski, J.; Stefanov, B. B.; Liu, G.; Liashenko, A.; Piskorz, P.; Komaromi, I.; Martin, R. L.; Fox, D. J.; Keith, T.; Al-Laham, M. A.; Peng, C. Y.; Nanayakkara, A.; Challacombe, M.; Gill, P. M. W.; Johnson, B.; Chen, W.; Wong, M. W.; Gonzalez, C.; Pople, J. A. *Gaussian 03*, revisions D-02 and E.01; Gaussian, Inc.: Wallingford, CT, 2004.
(14) *Jaguar*, version 6.5; Schrodinger, LLC: New York, 2005.
(15) Stephens, P. J.; Devlin, F. J.; Chabalowski, C. F.; Frisch, M. J. *J. Phys. Chem.* **1994**, *98*, 11623.
(16) Andrae, D.; Haussermann, U.; Dolg, M.; Stoll, H.; Preuss, H. *Theor. Chim. Acta* **1990**, *77*, 123.
(17) Tannor, D. J.; Marten, B.; Murphy, R.; Friesner, R. A.; Sitkoff, D.; Nicholls, A.; Ringnalda, M.; Goddard, W. A., III; Honig, B. *J. Am. Chem. Soc.* **1994**, *116*, 11875.
(18) Zeizinger, M.; Burda, J. V.; Sponer, J.; Kapsa, V.; Leszczynski, J. *J. Phys. Chem.* **2001**, *105*, 8086.
(19) (a) Stambuli, J. P.; Incarvito, C. D.; Bühl, M.; Hartwig, J. F. *J. Am. Chem. Soc.* **2004**, *126*, 1184. (b) Yamashita, M.; Hartwig, J. F. *J. Am. Chem. Soc.* **2004**, *126*, 5344.

Scheme 1

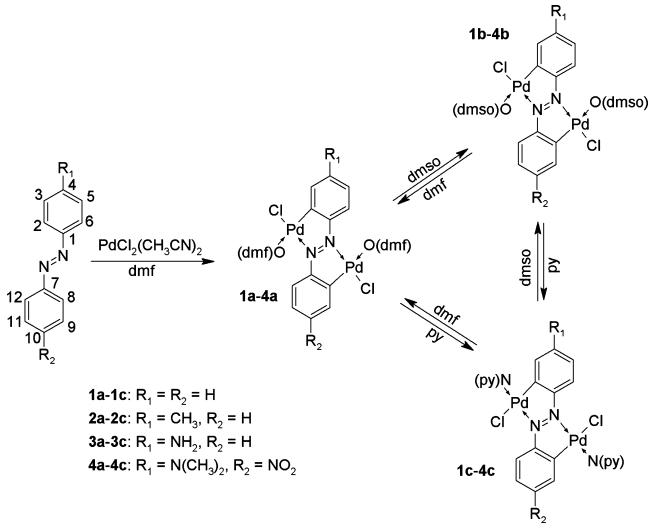

Figure S1) and ^{1}H NMR spectra confirm the loss of two molecules of DMF or DMSO from the initial complexes. The results of chemical analysis support the formulations of such species, either as coordinatively unsaturated T-shaped complexes or as polymers produced by chloride bridging. Although no definite conclusion can be made yet, the following facts indicate that the structure of the solvent free species is probably not T-shaped.

Unsaturated T-shaped palladium complexes have been prepared and structurally characterized by Hartwig et al.[19a,b] The structures of these complexes include agostic Pd···H−C interactions[20] and sterically hindered ligands at cis positions to the vacant coordinating site. If the solvent free species reported here were T-shaped monomers, they would be lacking both of these stabilizing features. Therefore, such a hypothesis does not appear likely. On the other hand, palladium complexes with chloride bridges are presently known only as dimers, for example, of monocyclopalladated azobenzenes,[1a,n] but dicyclopalladated azobenzenes seem to be quite capable of producing chainlike polymers.

Energy differences between coordinatively unsaturated T-shaped complexes and those including the solvent molecules were estimated by DFT calculations for a gas phase. Geometry optimization of T-shaped species produced only isomers with a vacant coordinating site at the trans position to the Pd−C bond, in agreement with previously known similar structures.[19a,b] The results (Table 2) indicate a greater stability of the complexes with solvent molecules and also make the hypothesis on the T-shaped species unfavorable. However, the energy differences are relatively small and comparable to the accuracy of ab initio calculations (1−2 kcal/mol). Further, the values in Table 2 indicate that the solvent molecules should be most easily removed from the pyridine complexes, which is in apparent disagreement with experimental findings. This inconsistency could be related to some unaccounted solid-state

Table 2. Free Energy Differences $\Delta G = G$(complex) − G(T-shaped)[a] − 2G(solvent), in kcal/mol, with Basis Set Superposition Correction Included, and without Translations and Rotations in G(complex) and G(T-shaped)

complex	ΔG	complex	ΔG	complex	ΔG
1a	−4.2	**1b**	−7.7	**1c**	−1.8
2a	−3.3	**2b**	−6.9	**2c**	−0.7
3a	−1.7	**3b**	−5.2	**3c**	+0.8
4a	−5.6	**4b**	−9.2	**4c**	−3.8

[a] Optimized geometries of T-shaped complexes are listed in SI Tables S54−S57.

effect, and until it is resolved, the computational results may have only informative value.

Experimental and calculated IR spectra of **1a** are in very good agreement (Supporting Information Figure S1). The experimental spectrum of the solvent free species obtained from **1a** and the calculated spectrum of the corresponding T-shaped complex roughly coincide, but they also markedly differ in the ranges 300−400 cm^{-1}, with two Pd−Cl stretchings of the T-shaped complex, and 1000−1100 cm^{-1}, with triangular deformations of the aromatic rings combined with Pd−C stretchings. Notably, the experimental spectra of **1a** and the corresponding solvent free species differ almost only in vibrations that can be assigned to DMF molecules in **1a**. One may hardly expect that the IR spectrum of the three coordinate T-shaped complex would differ from the common tetracoordinate complex only in terms of the missing vibrations of the solvent molecule.

Due to the complexity of polymeric structures, it is difficult to examine the alternate hypothesis on the polymeric nature of the solvent free species. No other experimental evidence for the specific formulation of these compounds could be obtained so far.

NMR Spectra. ^{1}H NMR spectra of complexes **2b** and **4b** confirmed double cyclopalladation of 4-methylazobenzene and 4-(dimethylamino)-4′-nitroazobenzene. All aromatic protons in these complexes are nonequivalent due to a loss of the ortho proton from each phenyl ring. Consequently, seven and six signals of aromatic protons were observed in ^{1}H NMR spectra of **2b** and **4b**, respectively (Experimental Section and Supporting Information Figure S2). The signals of ortho protons H-6 and H-12 and meta protons H-3 and H-9 are shifted downfield relative to the free ligand signal. A large downfield shift of these signals could be a consequence of intramolecular hydrogen bonds between ortho hydrogens (H-6 and H-12) and oxygen atoms of DMF (or DMSO) as well as between meta protons (H-3 and H-9) and chlorine atoms, as indicated by X-ray structures of the complexes. Double cyclopalladation of azobenzenes also causes an upfield shift of meta protons H-5 and H-11 and para protons H-4 and H-10 (where present). The same effect was observed for analogous protons in single cyclopalladated azobenzenes.[1j,k,m,21] The ^{1}H NMR spectra confirmed the presence of two solvent ligands (DMF, DMSO, or py) in each complex. These ligands could be oriented trans or cis toward the Pd−C bond, but only one set of signals was observed in the spectra of complexes, indicating that only

(20) Espinet, P.; Echavarren, A. M. *Angew. Chem., Int. Ed. Engl.* **2004**, *43*, 4704.

(21) Ćurić, M.; Tušek-Božić, Lj.; Vikić-Topić, D; Scarcia, V.; Furlani, A.; Balzarini, J.; De Clercq, E. *J. Inorg. Biochem.* **1996**, *63*, 125.

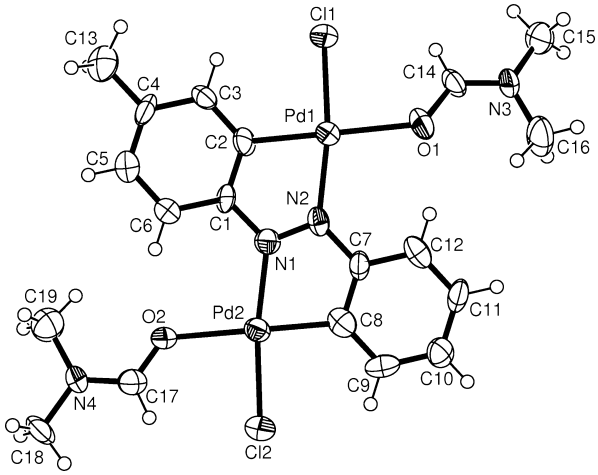

Figure 1. Molecular structure of **2a**. Thermal ellipsoids are shown at 50% probability, and hydrogen atoms are depicted as spheres of arbitrary radii. Possible hydrogen bonds C(6)−H···O(2) 2.977, 2.103 Å, 156°; C(17)−H···Cl(2) 3.164, 2.589 Å, 120°; C(9)−H···Cl(2) 3.195, 2.636 Å, 119°; C(12)−H···O(1) 2.984, 2.106 Å, 157°; C(14)−H···Cl(1) 3.224, 2.640 Å, 121°; and C(3)−H···Cl(1) 3.144, 2.569 Å, 120°.

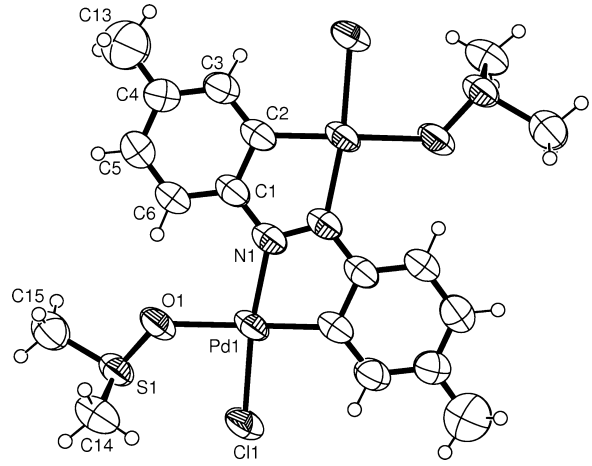

Figure 2. Molecular structure of **2b**. Thermal ellipsoids are shown at 50% probability, and hydrogen atoms are depicted as spheres of arbitrary radii. Possible hydrogen bonds C(6)−H···O(1) 2.927, 2.071 Å, 152°; C(14)−H···Cl(1) 3.606, 3.025 Å, 120° and C(3′)−H···Cl(1) 3.184, 2.639 Å, 117°.

one of them is present in solution. The signals of azobenzene protons in spectra of the complexes with py could not be assigned due to overlapping with signals of the pyridine protons. ^{13}C NMR spectra could not be obtained due to the low solubility of **2a**−**2c**, or due to the decomposition of **4a**−**4c** at concentrations above 10^{-4} mol dm^{-3}.

Crystal Structures. Crystal structures of the **1c**, **2a**,**b**, and **4a**,**b** complexes are shown in Figures 1−5 with the selected bonds and angles given in Table 3. All complexes contain two palladium atoms bridged by the azobenzene ligand acting as a double-chelating C,N donor. Consequently, two five-membered chelate rings are formed. Each palladium atom is additionally bound to chloride and the solvent ligand. The bond lengths and angles are within the range of values observed in analogous structures of **1a**,**b** and **3b**.[2,22] The azobenzene skeletons and Pd atoms have almost a planar arrangement, and the average deviation from the plane is

(22) Molčanov, K.; Ćurić, M.; Babić, D.; Kojić-Prodić, B. *J. Organomet. Chem.* **2007**, *692*, 3874.

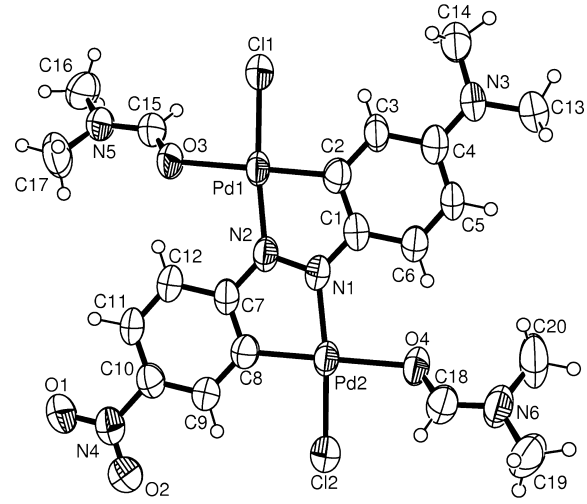

Figure 3. Molecular structure of **4a**. Thermal ellipsoids are shown at 50% probability, and hydrogen atoms are depicted as spheres of arbitrary radii. Possible hydrogen bonds C(6)−H···O(4) 2.912, 2.050 Å, 153°; C(18)−H···Cl(2) 3.209, 2.708 Å, 115°; C(9)−H···Cl(2) 3.209, 2.658 Å, 119°; C(12)−H···O(3) 2.977, 2.112 Å, 154°; C(15)−H···Cl(1) 3.215, 2.834 Å, 106°; and C(3)−H···Cl(1) 3.181, 2.603 Å, 121°.

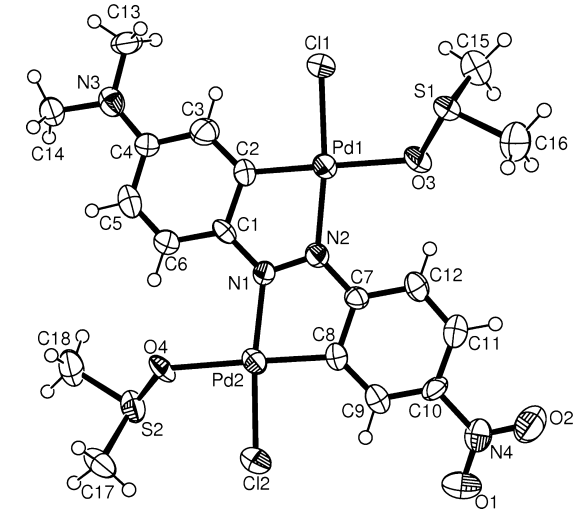

Figure 4. Molecular structure of **4b**. Thermal ellipsoids are shown at 50% probability, and hydrogen atoms are depicted as spheres of arbitrary radii. Possible hydrogen bonds C(6)−H···O(4) 2.977, 2.128 Å, 151°; C(9)−H···Cl(2) 3.168, 2.604 Å, 120°; C(12)−H···O(3) 2.940, 2.112 Å, 148°; and C(3)−H···Cl(1) 3.202, 2.650 Å, 119°.

below 0.1 Å, with the exception of Pd atoms in **1c**, which deviate from the azobenzene plane by 0.15 Å. Each palladium center is in a slightly distorted square-planar coordination mode. In complexes **2a**,**b** and **4a**,**b**, all five atoms lie within 0.1 Å from their plane, and within 0.2 Å in **1c**.

Depending on the trans or cis orientation of solvent ligands toward the Pd−C bond, two isomers are possible. Crystal structures of the complexes show that the DMF and DMSO ligands are coordinated through the O atom and oriented trans to the Pd−C bond in **2a**,**b** and **4a**,**b** as well as in **1a**,**b** and **3b**,[2,22] whereas the py ligands are cis-located in **1c**, Figures 1−5. Quantum chemical calculations indicate that the cis configuration is more stable in the complexes with pyridine (see below). The bond lengths between Pd and donor atoms (O or Cl) at the trans position are significantly longer than the values predicted from their covalent radii as a conse-

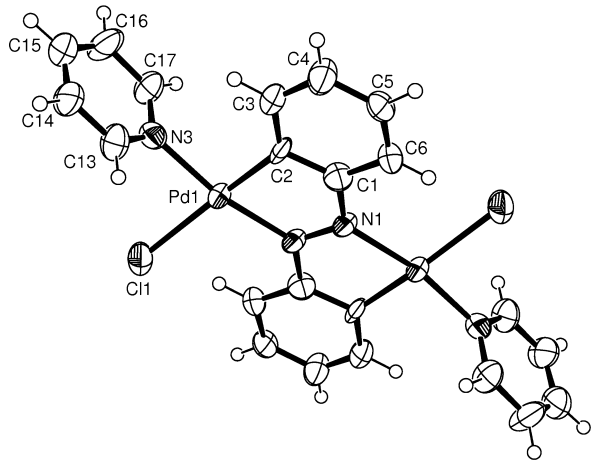

Figure 5. Molecular structure of **1c**. Thermal ellipsoids are shown at 50% probability, and hydrogen atoms are depicted as spheres of arbitrary radii. Possible hydrogen bonds C(3)−H···N(3) 3.034, 2.541 Å, 111° and C(6′)−H···Cl(1) 3.217, 2.431 Å, 142°.

Table 3. Bond Distances (in Angströms) and Bond Angles (in Degrees) around Pd Atoms from X-Ray Diffraction

	2a	4a	2b[a]	4b	1c
Pd1−C2	1.954(10)	1.925(7)	1.933(7)	1.917(15)	1.946(14)
Pd1−N2	2.054(14)	2.062(7)	2.054(5)	2.066(13)	2.046(10)
Pd1−Cl1	2.295(4)	2.309(2)	2.3055(16)	2.310(4)	2.407(4)
Pd1−O/N	2.189(14)	2.170(6)	2.159(5)	2.173(12)	2.047(10)
Pd2−C8	1.981(12)	1.962(7)		1.921(15)	
Pd2−N1	2.072(14)	2.063(6)		2.061(13)	
Pd2−Cl2	2.288(4)	2.300(2)		2.293(4)	
Pd2−O/N	2.201(12)	2.162(6)		2.148(10)	
C2−Pd1−N2	78.4(5)	79.2(3)	79.5(2)	80.7(6)	79.4(4)
N2−Pd1−O/Cl1	101.7(5)	100.6(2)	99.90(18)	99.0(5)	104.2(3)
O/N−Pd1−Cl1	87.0(3)	85.98(15)	87.58(12)	87.6(3)	85.6(3)
N/Cl1−Pd1−C2	93.3(3)	94.2(2)	93.23(16)	92.9(5)	92.0(4)
N2−Pd1−N/Cl1	170.6(4)	173.01(15)	172.39(14)	172.5(4)	169.3(4)
C2−Pd1−O/Cl1	175.3(5)	178.8(3)	173.3(2)	177.9(6)	166.1(4)
C8−Pd2−N1	78.3(5)	79.5(3)		80.5(6)	
N1−Pd2−O/Cl2	101.9(5)	100.3(2)		100.8(4)	
O/N−Pd2−Cl2	86.7(3)	86.7(2)		86.4(3)	
N/Cl2−Pd2−C8	93.2(3)	93.8(2)		92.3(5)	
N1−Pd2−N/Cl2	171.3(4)	171.79(15)		172.7(4)	
C8−Pd2−O/Cl2	176.0(5)	177.1(2)		174.9(6)	

[a] Geometry parameters obtained from X-ray diffraction around Pd1 and Pd2 in **2b** are equal due to pseudosymmetry of the crystal structure.

quence of the strong trans influence[23] of the C donor, Supporting Information Table S1.

In contrast to complexes **2a**,**b** and **4a**,**b**, complex **1c** has C_i molecular symmetry, Figure 1. Although lacking the molecular C_i symmetry, the complex **2b** of 4-methylazobenzene with DMSO as a solvent ligand lies also on the crystallographic inversion center at the midpoint of the N═N bond due to structural disorder, resulting in two opposite orientations of the molecule over the inversion center, with p.p. = 0.50. This effect was also observed in the analogous complex of 4-aminoazobenzene, **3b**.[2]

The X-ray structures of all complexes confirm that azobenzenes are indeed doubly cyclopalladated even when the strong polarized 4-(dimethylamino)-4′-nitroazobenzene, which contains electron-releasing and electron-withdrawing

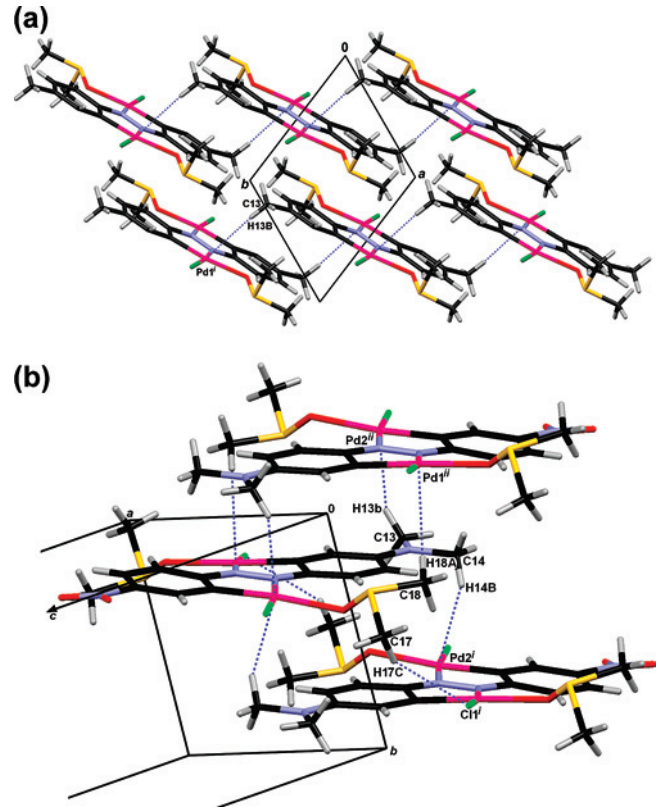

Figure 6. C−H···Pd hydrogen bonds in crystal packing of (a) **2b** and (b) **4b**. Symmetry operators are (*i*) $1-x, 2-y, -z$; (*ii*) $-x, 1-y, -z$, (*iii*) $-x, -y, -z$.

4,4′-substituents, is used as a ligand. Crystal structures of complexes **4a**,**b** with this ligand are the first direct proof that cyclopalladation may take place at the azobenzene ring with a strong electron-withdrawing substituent in the para position. A doubly cyclopalladated azobenzene complex with a similar combination of electron-releasing (dimethylamino) and electron-withdrawing (sulfonic) groups has been reported recently,[24] but without direct structural evidence.

The crystal structures of all complexes reveal 2D or 3D supramolecular assemblies with molecular components self-organized by C−H···Pd, C−H···Cl−Pd, C−H···π, or $\pi\cdots\pi$ interactions. In contrast to other interactions, C−H···Pd ones are found only in **2b** and **4b**, having C···Pd distances of 3.52(2)−3.92(2) Å, Figure 6 and Supporting Information Table S13. Athough it is known that electron-rich metal ions with a low coordination number (most typically Pt) can act as proton acceptors in a weak hydrogen bond,[25] only a few such bonds with palladium as an acceptor have been documented so far.[26a,b] Geometric parameters of all interactions and description of the crystal packing are given in the Supporting Information, section 1.

cis/trans Isomerism. In order to explain cis/trans isomerism at the binding position of solvent molecules, molecular

(23) (a) Rüttimann, S.; Bernardinelli, G.; Williams, A. F. *Angew. Chem., Int. Ed. Engl.* **1993**, *32*, 392. (b) Vicente, J.; Chichote, M. T.; Lagunas, M. C.; Jones, P. G.; Bembenek, E. *Organometallics* **1994**, *13*, 1243. (c) Vicente, J.; Areas, A.; Bautista, D.; Jones, P. G. *Organometallics* **1997**, *16*, 2127.

(24) Li, S.-H.; Yu, C.-W.; Xu, J.-G. *Chem. Commun.* **2005**, 450.

(25) (a) Desiraju, G. R.; Steiner, T. *The Weak Hydrogen Bond*; Oxford University Press: Oxford, U.K., 1999. (b) Braga, D.; Grepioni, F.; Desiraju, G. R. *Chem. Rev.* **1998**, *98*, 1375. (c) Brammer, L. *Dalton Trans.* **2003**, 3145.

(26) (a) Alyea, C.; Ferguson, G.; Kannan, S. *Chem. Commun.* **1998**, 345. (b) Vicente, J.; Abad, J.-A.; Frankland, A. D.; López-Serrano, J.; Ramírez de Arellano, M. C.; Jones, P. G. *Organometallics* **2002**, *21*, 272.

Table 4. Free Energy Differences G(trans) − G(cis) (in kcal/mol) between the cis and trans Isomers for Geometries Optimized in a Vacuum and in the Solvent (DMSO)

	vacuum[a]	solvent[b]		vacuum[a]	solvent[b]		vacuum[a]	solvent[b]
1a	−11.0	−9.0	**1b**	−9.1	−5.7	**1c**	−3.0	1.0
2a	−10.7	−7.1	**2b**	−9.6	−6.5	**2c**	−3.3	0.4
3a	−10.8	−7.0	**3b**	−9.4	−5.1	**3c**	−3.6	0.5
4a	−8.9	−8.8	**4b**	−8.0	−5.6	**4c**	−2.3	1.1

[a] Optimized geometries are listed in Supporting Information Tables S6−S29. [b] Optimized geometries are listed in Supporting Information Tables S30−S53.

geometries and energies were calculated for both isomers. Several conformers were found for most of the species, with slightly different orientations of the solvent molecule and the free energy differences always below 1 kcal/mol. The calculated structures are in reasonable agreement with X-ray structures. The experimental and calculated geometrical parameters around Pd atoms are listed in Supporting Information Table S1.

For comparison of the cis and trans isomers, only the most stable conformers were considered. In a vaccum, isomers with the solvent ligand at the trans position turned to be more stable. Remarkably, cis/trans energy differences for the py complexes are smaller than for complexes with DMF or DMSO (Table 4). After solvation has been accounted for, the cis isomers of the py complexes were found to be more stable than the trans isomers, in agreement with the experimental findings. The cis isomers are stabilized by solvation more than the trans isomers, and due to a small energy difference between the py isomers in a vacuum, solvation reverses the stability order only for these complexes. Therefore, the exhibited cis/trans isomerism can be explained only by taking into account both the differences in electronic structures of cis/trans isomers and the different amounts of their stabilization by the solvent. This finding agrees very well with the recent discussion[27] on the factors controlling relative stabilities of cis and trans isomers.

The trans influence[28] was also confirmed by the calculations. In all cases, Pd−Cl and Pd−(O/N) bonds in the trans arrangement to the Pd−C bond were about 0.12 Å longer than the corresponding bonds in the cis position.

Aromaticity of Palladium Rings. Structures of dicyclopalladated complexes contain four linearly fused rings. The outermost two are azobenzene phenyl rings, and the inner two rings (metallacycles) are formed by bridging the ligand with Pd−C and Pd−N bonds. These bonds prevent rotation of the phenyl rings and enforce coplanarity of the fused rings. Since metallacycles include conjugated C═C and N═N bonds, it is reasonable to assume that these rings also possess some aromatic character.

The aromaticity of five-membered palladacycles has been previously studied by using the variation coefficient of the bond orders V[29a] and HOMA[29b] indices in correlation to the ring planarity and Pd−N distance.[29c] V and HOMA for palladacycles in **1b**−**4b** azobenzenes were derived from the crystal structures and parameters in ref 29c. Mean values (ranges) of V and HOMA are 15.19 (11.59−17.53) and 0.75 (0.68−0.81), respectively, corresponding to more aromatic palladacycles.[29c] Since these indices measure the extent of delocalization in the ring bonds (indicated by bond lengths), it is informative to compare bond lengths in the free azobenzene ligand[30] with those in the cyclopalladated complex. All three common bonds (C═C, C−N, and N═N) are more delocalized in the complex than in free azobenzene. Another indicator of extended delocalization is the increased shielding of ^{15}N in the monocyclopalladated azobenzene derivative.[31] The chemical shift of the azo-nitrogen not connected to palladium is decreased relative to the free ligand (100.2 vs 118.0 ppm). A similar reduction is found for the ^{13}C in benzene and butadiene (128.4 vs 137.8 ppm).

A recently proposed aromaticity index[32] is based on the component of a shielding tensor (nucleus independent chemical shift, NICS) that is orthogonal to the ring plane. Particularly indicative are its values calculated for a range of increasing distances from ring. These NICS profiles are in good correlation with empirical data on aromaticity in various molecules.[32] Profiles calculated for complexes **1b**, **3b**, and **4b** (SI Figure S3) show remarkable difference between phenyl rings and palladacycles. NICS-profile for the latter is different both from typical aromatic (benzene) and typical antiaromatic system (cyclobutadiene), and most similar to the profile obtained for butadiene.[32] To estimate effect of a ring closure by binding metal to ligand, NICS-profiles for complexes were compared with those obtained for free ligands. A point nearby the ligand corresponding to the center of a given palladacycle in the complex, was determined as a centroid of an hypothetical ring that would be closed by binding the metal to the C and N atoms at the same distances as in the complex.

The obtained NICS profiles for pure ligands are qualitatively the same as those calculated for complexes (SI Figure S3). These results indicate that aromaticity of the palladacycles, characterized by NICS profile, is practically absent in comparison to the phenyl rings. Overall, one may conclude that cyclopalladation increases delocalization in the ligand part of the ring, but without establishing ring aromaticity.

UV−Vis Spectra and Excited Singlet States Calculations. UV−vis spectra of complexes **1b**−**4b** are shown in Figures 7−9 and in Supporting Information Figure S4, with the results of excited singlet-states calculations. The calculated excited states are listed in Table 5 (the first 10 excited states are shown; a complete list, including all 32 calculated states, is in Supporting Information Tables S2−S5). UV−vis spectra of azobenzene ligands are characterized by intense $\pi \rightarrow \pi^*$ transitions, increasingly shifted to longer wavelengths in the sequence: (**ab**, **mab**) < **aab** < **dmanab**. The

(27) Harvey, J. N.; Heslop, K. M.; Orpen, A. G.; Pringle, P. G. *Chem. Comm.* **2003**, 278.
(28) Appleton, T. G.; Clark, H. C.; Manzer, L. E. *Coord. Chem. Rev.* **1973**, *10*, 335.
(29) (a) Bird, C. W. *Tetrahedron* **1985**, *41*, 1409; **1986**, *42*, 89. (b) Krygowsky, T. M. *J. Chem. Inf. Comput. Sci.* **1993**, *33*, 70. (c) Krygowsky, T. M.; Ciesielski, A.; Bird, C. W.; Kotschy, A. *J. Chem. Inf. Comput. Sci.* **1995**, *35*, 203. (d) Crispini, A.; Ghedini, M. *J. Chem. Soc., Dalton Trans.* **1996**, 75.
(30) Brown, C. J. *Acta Crystallogr.* **1966**, *21*, 146.
(31) Tušek-Božić, Lj.; Ćurić, M.; Vikić-Topić, D.; Lyčka, A. *Collect. Czech. Chem. Commun.* **1997**, *62*, 1888.
(32) Stanger, A. *J. Org. Chem.* **2006**, *71*, 883.

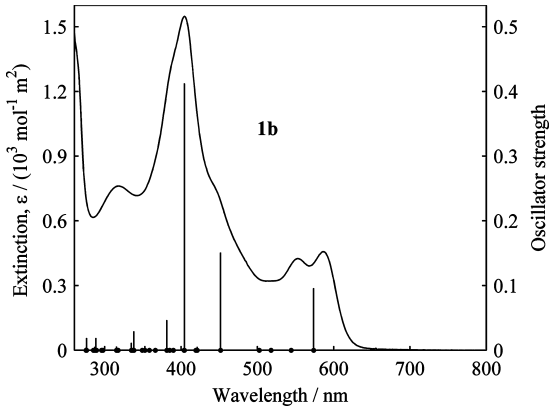

Figure 7. UV−vis spectrum of **1b** (recorded in DMSO). Bold dots on the apscisa denote calculated transitions from the ground to excited singlet states; heights of vertical lines correspond to oscillator strengths.

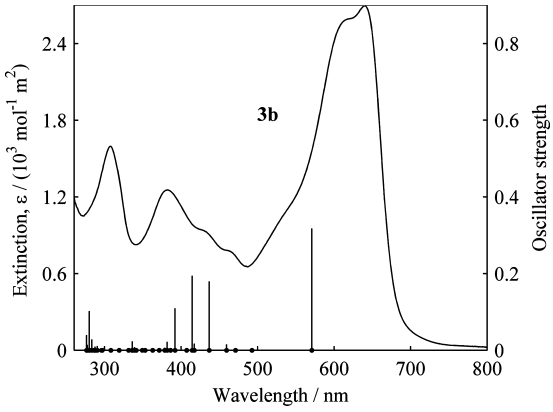

Figure 8. UV−vis spectrum of **3b** (recorded in DMSO). Bold dots on the apscisa denote calculated transitions from the ground to excited singlet states; heights of vertical lines correspond to oscillator strengths.

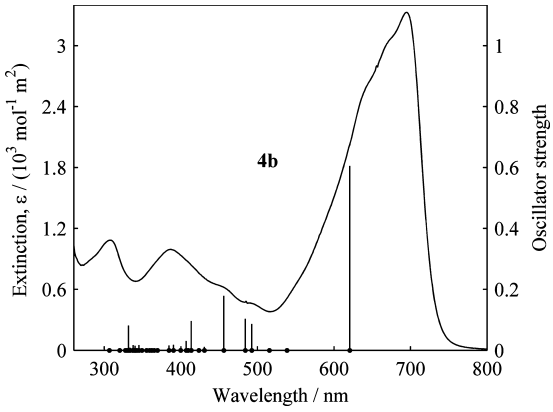

Figure 9. UV−vis spectrum of **4b** (recorded in DMSO). Bold dots on the apscisa denote calculated transitions from the ground to excited singlet states; heights of vertical lines correspond to oscillator strengths.

lowest transition is $n \rightarrow \pi^*$, which is symmetry-forbidden in azobenzene and has low intensity in asymmetrically substituted derivatives.[33] Only for **dmanab** do TD-DFT calculations indicate that solvation effects (in DMSO) move $\pi \rightarrow \pi^*$ transition to the lowest energy, so that $n \rightarrow \pi^*$ becomes the second excited state. In monocyclopalladated azobenzenes,[1h,j,m] the absorption bands corresponding to the lowest transition energies are also red-shifted in the same order as with free ligands. TD-DFT calculations show that these transitions have $\pi \rightarrow \pi^*$ character.

(33) Bisle, M.; Römer, M.; Rau, H. *Ber. Bunsen. Physik. Chem.* **1976**, *80*, 301.

Table 5. Wavelengths (*w*/nm), Oscillatory Strengths (*f*), and Description of Charge Redistribution for Electronic Transitions from Ground to Lowest 10 Excited States of **1b**−**4b**, Calculated by TD-DFT

exc. state		1b	2b	3b	4b
1	*w*	573.6	570.2	570.8	620.6
	f	0.10	0.13	0.32	0.61
		IL[a]($\pi-\pi^*$)	IL($\pi-\pi^*$)	IL($\pi-\pi^*$)	IL($\pi-\pi^*$)
2	*w*	544.2	535.2	492.6	538.2
	f	0.00	0.00	0.00	0.00
		MLCT[b]	MLCT	MLCT	MLCT
3	*w*	517.9	509.9	471.0	515.3
	f	0.00	0.00	0.00	0.01
		MLCT	MLCT	MLCT	MLCT
4	*w*	502.3	495.3	459.3	492.6
	f	0.00	0.00	0.02	0.09
		MLCT + IL	MLCT + IL	MLCT + IL	MLCT + IL
5	*w*	451.7	448.0	436.8	484.0
	f	0.15	0.14	0.18	0.10
		MLCT + IL	MLCT + IL	MLCT + IL	MLCT + IL
6	*w*	421.0	418.6	417.1	455.9
	f	0.01	0.08	0.02	0.18
		mixed	IL($\pi-\pi^*$) + MLCT	LMCT[c] + IL($\pi-\pi^*$)	MLCT
7	*w*	419.4	416.0	414.4	430.6
	f	0.00	0.00	0.19	0.01
		mixed	mixed	IL($\pi-\pi^*$) + MLCT	IL($\pi-\pi^*$)
8	*w*	404.3	407.2	407.3	423.5
	f	0.41	0.37	0.00	0.01
		IL($\pi-\pi^*$) + MLCT	IL($\pi-\pi^*$) + MLCT	LMCT + IL($\pi-\pi^*$)	mixed
9	*w*	404.0	399.9	392.0	413.4
	f	0.00	0.00	0.11	0.10
		mixed	mixed	IL($\pi-\pi^*$) + MLCT	mixed
10	*w*	389.8	391.1	386.2	409.4
	f	0.00	0.00	0.00	0.00
		LMCT + IL($\pi-\pi^*$)	LMCT + IL($\pi-\pi^*$)	mixed	IL($\pi-\pi^*$) + LMCT

[a] IL = charge redistribution within the azobenzene ligand. [b] MLCT = charge transfer from Pd atoms to the azobenzene ligand. [c] LMCT = charge transfer from the azobenzene ligand to Pd atoms.

In dicyclopalladated complexes **1b**−**4b**, the lowest transitions are shifted to lower energies in the same order as in monocyclopalladated species, but with higher intensity. TD-DFT calculations show that this is $\pi \rightarrow \pi^*$ transition, with well-reproduced changes in intensity. Yet, the wavelength shift is only qualitatively reproduced for **4b**, while for **3b**, the lowest transition energy stays close to that for **1b**. This remains unchanged if B3LYP was replaced with PBE0, or the basis set was enlarged. It could be that specific interactions with the solvent are reponsible for the shift in **3b**, perhaps contributing also to the shift in **4b**. The next four transitions in **1b**−**4b** have common density redistribution features with a significant amount of metal-to-azobenzene ligand charge transfer (MLCT) and more (fourth and fifth excited states) or less (second and third) $\pi \rightarrow \pi^*$ intraligand density redistribution (Table 5). The most intense transitions from the ground state in **1b** and **2b** are to the eighth excited state, with dominant intraligand $\pi \rightarrow \pi^*$ character and small admixture of MLCT. In **3b** and **4b**, the most intense are transitions to the first excited state, and then to the seventh

and sixth excited states, respectively, having mostly MLCT character with greater contribution from the Pd2 atom.

Complexes **3b** and **4b** show some fluorescence activity in DMSO. Complex **3b** emits at 670 and 720 nm, with an excitation wavelength at 640 nm, while **4b** emits at 640 nm when it is excited at 590 nm, and at 720 nm when excited at 700 nm.

Acknowledgment. The Ministry of Science, Education and Sports of The Republic of Croatia (Grant Nos. 098-0982915-2950 and 098-1191344-2943) provided financial support for this research. Computations were done on the Isabella cluster at SRCE, Zagreb. Discussions with Dr. Ivan Ljubic and Dr. David M. Smith are gratefully acknowledged.

Supporting Information Available: Crystal structure data of **1c**, **2a**,**b**, and **4a**,**b** (CIF files); description of crystal packings; IR spectra of **1a** and the corresponding solvent free compound; NMR spectra of **2a** and **4b**; NICS profiles for **1b**, **3b**, and **4b**, and for ligands **ab**, **aab**, and **dmanab**; calculated geometries and energies of all isomers in a vacuum and in solution; complete listing of computed excited states. This material is available free of charge via the Internet at http://pubs.acs.org.

IC8010234